Influence of water vapour on the propagation speed and mean energy of an atmospheric non-equilibrium diffuse discharge in air

Conference Paper · July 2017

CITATIONS
0

READS
59

8 authors, including:

Kristaq Gazeli
Université Paris 13 Nord
46 PUBLICATIONS **317** CITATIONS
SEE PROFILE

Karim Ouaras
École Polytechnique
18 PUBLICATIONS **92** CITATIONS
SEE PROFILE

Lionel Magne
French National Centre for Scientific Research
71 PUBLICATIONS **887** CITATIONS
SEE PROFILE

S. Pasquiers
French National Centre for Scientific Research
139 PUBLICATIONS **1,518** CITATIONS
SEE PROFILE

Influence of water vapour on the propagation speed and mean energy of an atmospheric non-equilibrium diffuse discharge in air

A. Brisset[1], P. Tardiveau[1], K. Gazeli[1], B. Bournonville[1], P. Jeanney[1], K. Ouaras[1], L. Magne[1], S. Pasquiers[1]

[1]*Laboratoire de Physique des Gaz et des Plasmas, Paris-Saclay University, CNRS, Orsay, 91400, France*

Abstract: We report results on the influence of humidity on the propagation and the energy of a pin-to-plane nanosecond pulse discharge at atmospheric pressure. Water vapour only impacts discharges in saturated gas mixtures, for which propagation is first slowed down, but accelerates faster than usual close to the plane. Energy is unchanged.

Keywords: Non-equilibrium atmospheric air plasma, nanosecond discharges, humidity effects, water saturation, fast imaging, optical emission spectroscopy

1. Introduction

This work comes within a research on the fundamental mechanisms of diffuse electric discharges and the associated non-equilibrium plasmas in air, at atmospheric pressure. Such discharges are created at very high over-voltages, several tens of kV, with sub-nanosecond rise times and without any pre-ionizing system [1]. At those over-voltages, the very structure of the discharge is modified: it is not filamentary anymore but diffuse, so the plasma covers a much larger gas volume. In these conditions, the over-voltage leads to more intense electric fields than those of the classic streamer discharges by promoting the Laplacien field as compared with the space charge field. The very high field values can then promote collisional mechanisms such as ionization, dissociation and molecular excitation [6], on much larger gas volumes than in the classical streamers.

Various applications are intended for this kind of discharges, among them air treatment, plasma-assisted combustion or other energetic applications [3-4]. These applications use gas mixtures containing different components such as water vapour or combustible and polluting molecules. Therefore, it is necessary to better understand the influence of such components on the development of the discharge. More specifically, this study deals with the influence of water vapour on the propagation speed and mean energy of a nanosecond pin-to-plane discharge in air at ambient temperature. Water is always present in uncontrolled environments and it is proved to have great influence on the discharge kinetics [5-6-7], notably for the production of potentially high amounts of radicals like OH and O [8]. Better understanding of the physical and chemical processes of these discharges are aimed to develop advanced and high energy efficiency reactors. The high field values that make large volume discharges, should enable the design of plasma reactors presenting more homogeneous properties than current ones.

The main aim of the present study is to demonstrate the effect of the presence of water vapour on the dynamics and energy of the discharge. Section 2 presents the experimental setup, the operating conditions of the discharge and the experimental methods applied. In section 3 are analysed the sub-nanosecond imaging measurements giving the discharge propagation speed and its energy, for each working condition. It also presents rotational temperature measurements obtained by emission spectroscopy of diatomic excited probe molecules. The experimentally determined plasma temperature will support kinetic models and it will help to reveal fundamental mechanisms (like the hydrodynamic expansion to be confirmed). The obtained results are discussed in section 4.

2. Experimental method

The diffuse nanosecond discharge is created in a pin-to-plane configuration of electrodes being separated by a gap of 19 mm. The pin is made of titanium with 100 µm curvature radius. The plane is an 8 cm radius copper plate. Positive high voltage nanosecond pulses, created by a FID-type technology power supply are applied to the pin (cf. figure 1). The plane is connected to the ground. The voltage rise time is 2 ns. Each experiment is done for three voltage amplitudes: 65, 75 and 85kV. The experiment is run at 5 Hz. A complete description of the device is presented in [10]. The electrodes are placed in a 1L/min flow of synthetic air into which water vapour is added up to 1.2, 2.0 or 2.2% through a controlled temperature water evaporator followed by a dilution system. To reach high concentrations of water vapour without any condensation

effects on cold spots of the gas line, two precautions were taken: first, it was ensured that the evaporator (placed in a temperature controlled bath) at least two degrees below the ambient temperature (about 23 °C). Second, the water saturated air was diluted at the exit of the evaporator.

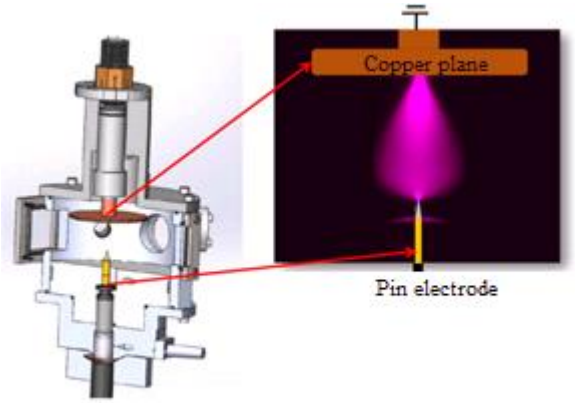

Fig. 1. Experimental setup and discharge visualisation.

To measure the propagation speed of the discharge, we used optical emission measurements based on fast imaging 4-Picos Stanford ICCD camera. The light was integrated in terms of the wavelength over the UV-visible spectrum, and integrated spatially over the whole discharge volume. However, it was temporally resolved. Hereafter, the imaging measurements characteristics: 200ps exposure time gate, images were recorded every 100ps or 300 ps. The time jitter was about 300ps [1]. Each image was averaged over 20 discharges. To get the speed of propagation, we need to define the position of the front of the discharge for each image. As the images are integrated on the line of sight of the camera, we ideally need to reconstruct the emission on the axial plane of the discharge. The Abel inversion is a relevant method in our case as the discharge is symmetric around the pin-to-plane axis. Based on this symmetry, the Abel treatment is able to reconstruct the profiles of the discharge in a plane including the symmetry axis [9], therefore the treatment is able to get to the local emission. However, as the front is located at the very tip of the discharge, where very little emission is integrated on the line of sight of the camera, the Abel inversion appeared in fact not necessary. We get the same propagation speed values before and after Abel processing. As the Abel processing requests a sophisticated treatment, the results presented herein were obtained without the Abel treatment. To define the precise location of the discharge front on the central axis, we choose an intensity threshold criterion. The same intensity threshold is used for each condition to get relevant interpretations.

The propagation speed uncertainties presented in the graphs are obtained using a linear regression method. They range between ± 0.07 and ±0.3 mm/ns. They are similar to the experimental uncertainties estimated on repeatability measurements, which range between ±0.1 and ±0.3 mm/ns.

The mean energy of the discharge is obtained by integrating the product of the current and the voltage over the discharge duration. The corresponding signals are plotted in figure 2, for a typical voltage pulse. Current and voltage signals are synchronized in time by paying special attention to the capacitive current (without discharge), based on the relation (1):

$$i_c = C\frac{dV}{dt} \quad (1)$$

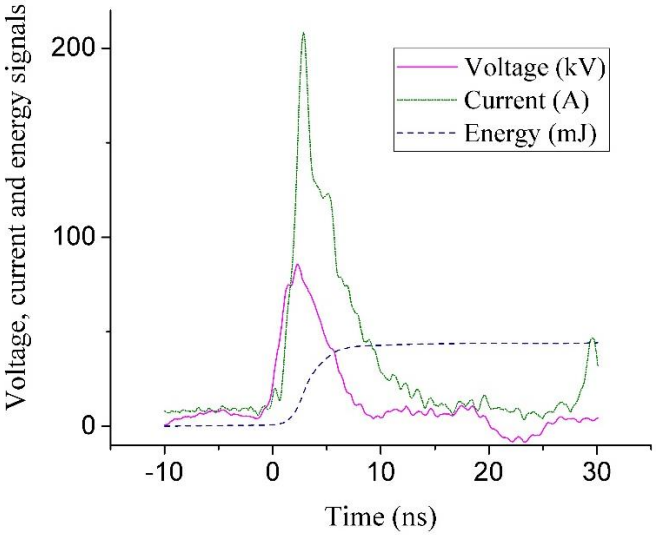

Fig. 2. Voltage, current and energy profiles for a typical voltage pulse of 85 kV.

Optical emission spectroscopy (OES) measurements have been carried out also to determine the mean rotational temperatures of the second positive system (C-B) of N_2. To get the temperature of the gas, we could not refer to the frequently used hypothesis that the rotational relaxation time of $N_2(C)$ is very small compared to its life time. Indeed, in our discharges the life time of $N_2(C)$ is about 0.7ns while its relaxation time is about 0.4ns. Both characteristic times are too close to conclude on the thermalization of $N_2(C)$. Another case allows the use of OES measurements of $N_2(C)$ which relies on the double equality: $T_{rot}(N_2(C)) \approx T_{rot}(N_2(X)) \approx T_{trans}(N_2(X))$ [13,18]. To assure the first equality, the electric field needs to be sufficiently high to consider that $N_2(C)$ is mainly created by electronic impact: $N_2(X) + e \rightarrow N_2(C) + e$. This is the case for our discharge [16]. This field condition is related to the work of Park [17] which demonstrates that if an excited species is created by electronic impact, the quantum number J is unchanged. Therefore, the rotational distribution of $N_2(C)$ is representative of the distribution of $N_2(X)$. In these high field and discharge conditions, we consider that: $T_{rot}(N_2(C)) = 0.92*T_{rot}(N_2(X))$ [13]. The second equality is confirmed as the rotation-translation time of $N_2(X)$ is about 0.4ns, which is much faster than the 10ns time of measurement. With these statements, we assimilate the measured rotational temperature of N_2(C-B) to the gas temperature. Then, we compared the experimental rotational distributions with the corresponding simulated ones, generated with a home-made code [11, 12].

Experiments were conducted using a 75 cm focal length imaging spectrometer (Acton SP 2750 PI) equipped with an ICCD camera (PI-MAX 2 of Princeton instruments) with a time gate resolution of 10 ns. A UV optical fibre is located

near the quartz window of the reactor to collect light perpendicularly to the plasma. We mainly use a 2400groove.mm^{-1} grating to maximize the spectral resolution (down to 0.04 nm). For rotational temperature determination, we use the emission of the (0,0) and (0,1) vibrational bands of N_2 (C-B), corresponding to the λ=337.13 nm and λ=357.69 nm transitions with a fitting procedure given by [13].

3. Results

Figure 3 depicts the positions of the discharge front on the central axis at different times and for three voltage amplitudes. The beginning of the discharge is chosen to coincide with the time when light emission is detected at the pin, while the end of the discharge coincides with the time when the discharge reaches the plane. For each characteristic pulse, the front positions are shown in dry air and for two water vapour concentrations: 1.2 % and 2.0 % or 2.2 %. We observe a linear propagation of the fronts during most of the discharge propagation time. Hereafter, we therefore consider the speed of the discharge to be constant on this time range and the speed values presented will only characterize this time range. Then, the propagation accelerates dramatically, until the discharge reaches the plane.

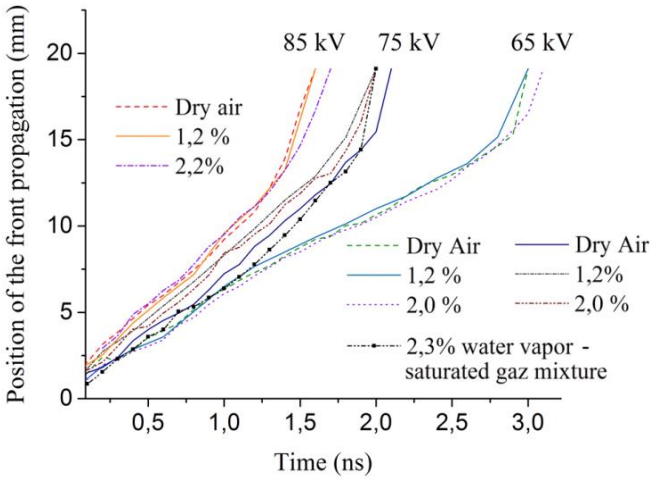

Fig. 3. Positions of the discharge front in time. The gas mixtures are dry air, air-water unsaturated mixtures at concentrations reaching 1.2 %, 2 % or 2.2 %, and water saturated air mixture (2.3 %).

Independently of the amplitude of the voltage, the experimental results show no modification of the discharge speed with the presence of water vapour, except if the air is saturated. At saturation conditions, the speed of the discharge is significantly lowered. Also to be noticed, at saturation, the final acceleration of the discharge seems surprisingly quicker than it is in the unsaturated gas.

Figure 4 depicts the influence of water vapour on the discharge propagation speed for different voltage amplitudes. The propagation speed is determined using a linear regression method, for a given gas mixture. Each point of the graph is an average over 2 to 5 experiments which determine the propagation speed as detailed in figure 3. The black /green/ blue/ red/ purple curve represent the propagation speed for each voltage amplitude in dry air /1.2%/ 2.0%/ 2.2% unsaturated water-vapour mixture/ 2.3% saturated water vapour mixture.

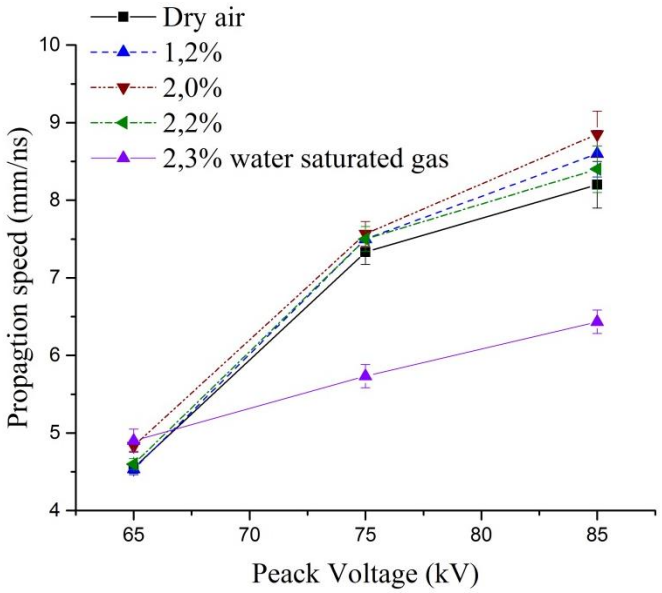

Fig. 4. Propagation speed of the discharge versus the peak voltage in dry air, in air-water vapour unsaturated mixtures (1.2%, 2.0%, 2.2% water concentrations) and in water-saturated mixture (2.3%).

The increasing uncertainty on the speed values with the voltage is due to the experimental method used: we kept the same 0.1 ns time interval between each acquisition, while the time of the discharge decrease at higher voltages. This resulted in fewer measures along the propagation which were accounted for the linear regression.

Electrons are the major species contributing to the propagation and the light emission of the discharge through the ionizing wave phenomena. Therefore, in a first approach, this work is limited to the study of electronic coefficients that could influence the discharge's propagation: electronic attachment, mobility and drift and diffusive coefficients. Simulations made with the BOLSIG+ tool [14] in unsaturated humid air show no significant modification of the three last coefficients for our estimated range of values of the reduced electric field (from 100 to 1000 Td). The electronic attachment increases significantly in humid air, but at fields higher than 100 Td it is negligible compared to the ionization coefficient. Then, the effective ionization coefficient, does not depend on humidity. Indeed, we observed no modification of the discharge propagation with humidity in the case of non-saturated gas. Now, in saturated air, another mechanism is probably to consider. At water saturation, LIF experipments, previously made at the LPGP under similar discharge conditions, revealed the presence of water molecule agregates. It is possible that the propagation of the discharge is modified due to the presence of this water agregates. Studies have already reported on the propagation of streamers in gases containing dust particles [15]. An increase of the propagation speed of the streamer in presence of dusts was measured. In our experiment however, the propagation speed is lowered in presence of water agregates. This is not necessarily contradictory. In reference [15], the size of the dusts ranges between 25 and 80 µm, while the size of the water agregates is expected to be of the nanometric scale. Furthermore, the dusts in reference [15] are

dielectrics that strenghten locally the electric field. It might not be the case with the water agregates. Several lines of inquiries are on study. For instance, the possibility of a modification of the electron attachment for water agregates, or the possibility of significant energy transfer during the collision of an electron and an agregate, which could lead to the break up of the agregate.

The results obtained on the mean energy of the discharge for a single voltage pulse, are presented in figure 5. We observe that the mean energy does not vary with water vapour concentration even for a saturated water-air mixture. At voltages close to 65kV, the mean energy is about 4.3mJ (±0.9mJ). At 75kV, it reaches at 15.6mJ (±0.7mJ) and at 85kV, 31.8mJ (±3.6mJ).

Even if the currents and the energies are high, the gas temperature remains low around 330 K. Figure 6 displays results of OES measurements on rotational temperatures of the (0,0) and (0,1) bands of the N_2(C-B) system.

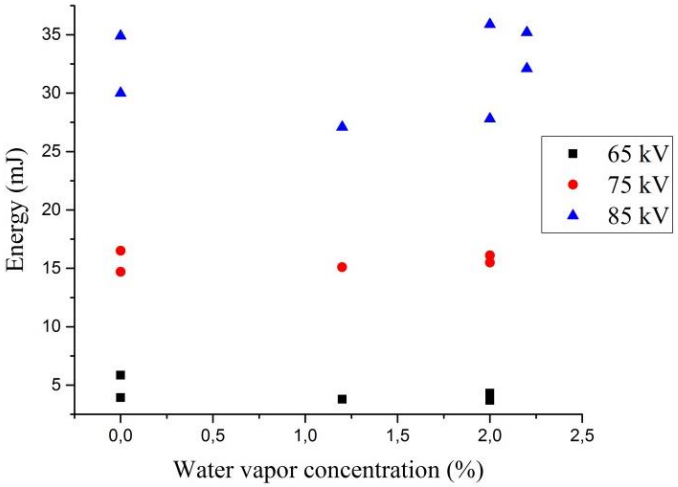

Fig. 5. Energy of the discharge versus water vapour concentration in the gas mixture for three voltages: 65kV, 75kV and 85kV.

We observe that, for spatial integration and 10 ns time average, there is no heating of the gas: its temperature remains close to 330 K ± 20 K independently of the water vapour concentration.

4.Conclusion

The present work provides preliminary data on the influence of up to 2,2% of water vapour in air at saturation conditions or unsaturated ones. Unless the gas mixture is saturated, there is no significant modification neither on the propagation speed of the discharge nor on the mean energy. However, for water saturated air, the speed is significantly lower, while the energy remains similar. Hypothesis about the modification of the electronic attachment in saturated air, or the possibility of energy transfer during electron and water aggregate collisions, can be evoked. Also, the acceleration of the propagation at the end of the discharge, seems to be faster under saturated air conditions.

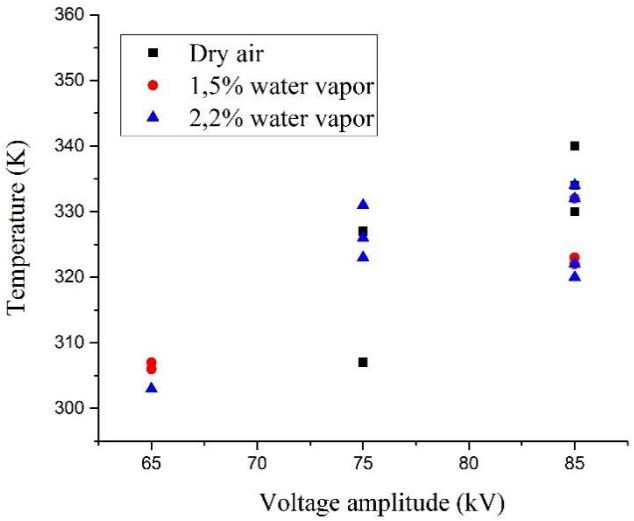

Fig. 6. Rotational temperatures of the (0,0) and (0,1) bands of the N_2(C-B) (λ=337.13nm and λ=357.69nm) in humid air and for different voltages (65, 75, 85 kV). The error is estimated to be ±20 K at 85 kV and 75 kV where the signal-to-noise ratio (S/N) is high and ±40 K at 65 kV, where the S/N ratio is low.

6.References

[1] P. Tardiveau, L. Magne, E. Marode, K. Ouaras, P. Jeanney and B. Bournonville, Plasma Sources Sci. Technol. 00 (2016) 000000 (16pp)

[3] J.M. Pouvesle, Proc. ISPC19 (2009) PL5

[4] C.D. Cathey, T. Tan, T. Shiraishi, T. Urushihara, A. Kuthi, and M. A. Gundersen, IEEE Trans. Plasma Sci. 35 (2007) 1664–1668

[5] J. T. Herron and D. S. Green, Plasma Chemistry and Plasma Processing, Vol. 21, No. 3, 2001

[6] L. W. Sieck, J. T. Herron and D. S. Green, Plasma Chemistry and Plasma Processing, Vol. 20, No. 2, 2000

[7] P. N. Mikropoulos, B. C. Sarigiannidou, C. A. Stassinopoulos and Ch. Tsakiridis, 40th Universities Power Engineering Conference, Cork, Ireland, 2005, Vol. 2.

[8] D. Singleton, C. Carter, S. J. Pendleton, C. Brophy, J. Sinibaldi, J. W. Luginsland, M. Brown, E. Stockman, M. A. Gundersen, Combustion and flame, volume 167, may 2016

[9] I. Beniaminy, M. Deutsch, Computer Physics Communications 27 (1982) 415—422

[10] P. Tardiveau, PSST, (submitted)

[11] K. Gazeli, P. Svarnas, B. Held, L. Marlin, F. Clement, *J. Appl. Phys.* **117**, 093302 (2015)

[12] R. P. Cardoso, T. Belmonte, P. Keravec, F. Kosior, and G. Henrion, *J. Phys. D: Appl. Phys.* **40**, 1394 (2007)

[13]D. L. Rusterholtz, D. A. Lacoste, G. D. Stancu, D. Z. Pai and C. O. Laux, J. Phys. D: Appl. Phys. 46(2013)464010(21pp)

[14] G.J.M. Hagelaar and L.C. Pitchford, Plasma Sci Sources and Tech 14, 722 (2005).

[15] N. Babaeva, A. N. Bhoj, M. Kushner, Plasma Sources Sci. Technol. **15** (2006) 591–602

[16] N. A. Popov, J. Phys. D: Appl. Phys. 44 285201 (2011)

[17] C. Park, *Nonequilibrium Hypersonic Aerothermodynamics* (New York: Wiley) (1989)

[18] F. Sainct, PhD Energy and Physics, Châtenay-Malabry, Central School of Paris (2014)